European Physical Journal A 58.4 (2022): 66

DOI: https://doi.org/10.1140/epja/s10050-022-00719-5

Weak binding effects on the structure of ^{40}Mg

A. O. Macchiavelli, H. L. Crawford, P. Fallon, and R. M. Clark
Nuclear Science Division, Lawrence Berkeley National Laboratory, Berkeley, CA 94720, USA

A. Poves
Departamento de Física Teórica and IFT-UAM/CSIC, Universidad Autónoma de Madrid, 28049 Madrid, Spain

(Dated: January 12, 2022)

While the phenomenon of one- and two-neutron ground-state halo nuclei is well established, the effects of weak binding on nuclear excitation properties remain largely unexplored. Motivated by this question and by recent data in ^{40}Mg we investigate the coupling of weakly bound (halo) valence neutrons to a core using the known properties of ^{40}Mg to explore and illustrate possible particle-core coupling schemes and their impact on the low-lying excitation spectrum.

I. INTRODUCTION

The properties of nuclei close to the neutron drip-line can differ from those near to stability due to the presence of weakly bound valence neutrons. One of the most striking structural changes to emerge is the formation of a neutron halo, where the outermost one or two weakly bound valence neutron states form a spatially extended surface comprised almost entirely of neutrons. As well as being near threshold the valence neutrons must also occupy low-ℓ states (s, p) to minimize the effects of an angular momentum barrier and allow their wavefunction to extend significantly beyond the core.

Focusing on two-neutron halos, first evidence came from a measurement of the interaction cross-section of ^{11}Li [1] reported in 1985. In their seminal work [2] Hansen and Jonson showed that the low binding in ^{11}Li leads to *neutronization* of the nuclear surface as originally suggested by Migdal [3], where the nucleus is surrounded by a neutron halo extending to several times the nuclear (core) radius. It is interesting to note that this state may be interpreted as a bound dineutron coupled to the nuclear core [3]. The extra attraction between the two neutrons in the presence of a Fermi sea gives rise to a bound *nn* structure despite the fact that the free di-neutron is not bound [4].

While the phenomenon of a one- and two-neutron ground-state halo is well established (there are over 10 known cases that have been experimentally confirmed, ranging from ^{6}He to ^{37}Mg) the effects of weak binding on nuclear structure properties remain largely unexplored. Motivated by this question and by recent data in ^{40}Mg [5] we investigate the coupling of weakly bound (halo) two valence neutrons to a core using the known properties of ^{40}Mg to explore and illustrate possible particle-core coupling schemes and their impact on the low lying excitation spectrum. ^{40}Mg lies close to the neutron drip line and is a potential candidate for a halo nucleus with two neutrons occupying the $p_{3/2}$ orbit [6–8], and where the observed spectrum of γ-ray transitions deviates from that seen in the neighboring more bound ^{36,38}Mg isotopes.

Of particular interest are the effects of the continuum on nuclear rotational motion. These have been studied in Ref. [9, 10] in the framework of the particle-plus-core problem using a non-adiabatic coupled-channel formalism. The subtle interplay between deformation, shell structure, and continuum coupling can result in a variety of excitations in an unbound nucleus just outside the neutron drip line, as predicted for the low-energy structure of ^{39}Mg.

In this work we take a more qualitative view, yet one that captures the main physical ingredients, to study the low-lying excitations that may emerge in a halo nucleus. We begin in Section II by discussing a "universal" plot that relates the $2n$ separation energy (S_{2n}) to the volume overlap between the core and halo as a way to characterize and identify possible halo nuclei, and then use the Weak Coupling [11] and Particle-Rotor Models [12] in a phenomenological approach in Section III, expanding on the scenarios first presented in Ref. [5].

II. CORE-VALENCE OVERLAP

As discussed in Ref. [2] and subsequent works [13–16] (see also the recent monograph [17]) the extended matter radius exhibited by a two-neutron halo nucleus can be expressed in terms of the separation energy of the weakly bound neutrons (S_{2n}) through the tunneling parameter $\mathscr{X} = r_c\sqrt{2\mu S_{2n}}/\hbar$ derived from the exponential nature of the asymptotic wavefunction. We thus consider a plot of $(< r_c^2 > / < r_m^2 >)^{1/2}$ vs. $\mathscr{X}$ as a way to capture the universal features of the $2n$ halo systems, where μ is the reduced mass of the core + 2n system, and r_c, r_m are the core and matter radii respectively. Their root-mean-square (RMS) ratio represents the volume overlap between the valence nucleons and core.

The experimental data on known $2n$ halo nuclei were obtained by comparing matter radii from Ref. [18] to a local $A^{1/3}$ fit of r_c in an isotopic chain for $\mathscr{X} > 1$. The results are shown in Fig. 1, where the two black curves are the expectation for $\ell = 0, 1$. The range of binding energy expected for ^{40}Mg is indicated by the shaded region. The mass table evaluation [19, 20] gives

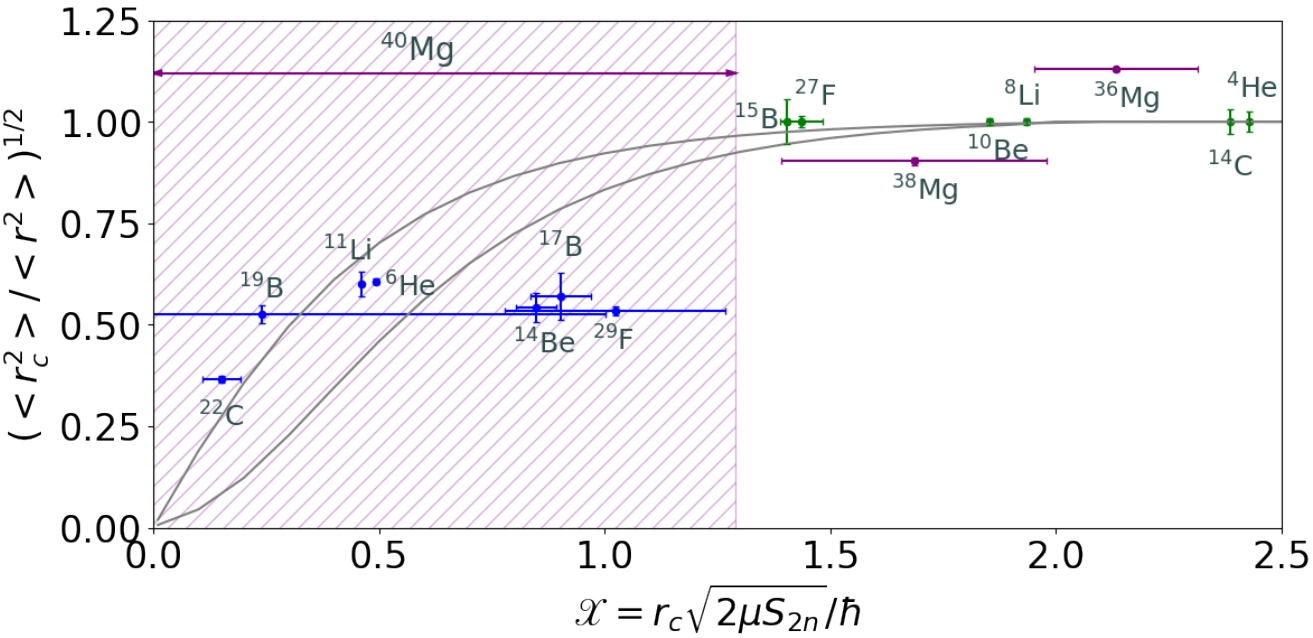

FIG. 1: Universal plot for $2n$ halos showing the dependence of $(< r_c^2 > / < r^2 >)^{1/2}$, a measure of the volume overlap, with the tunneling parameter $\mathscr{X}$. The black curves show the expected behavior for $\ell = 0, 1$. The blue data points correspond to known $2n$ halo nuclei, while the green data points were used for fitting the value of r_c. The purple data points correspond to the Mg isotopes.

an expected S_{2n} of 667 ± 706 keV. Within this range of binding energy we may expect a reduced core-valence overlap, suggesting that ^{40}Mg is a possible $2n$ halo candidate where, as we shall discuss, a (almost) spherical p^2 two-neutron halo may develop on top of a deformed ^{38}Mg core [8]. An inspection of the figure clearly suggests that in the future both mass and interaction cross-section measurements of ^{40}Mg will be crucial to firmly establish its (potential) halo nature.

III. PARTICLE-CORE COUPLING

The spatial separation between the two halo neutrons and the core suggests that the motion (excitation modes) of the system as a whole is reasonably described by that of the individual subsystems and the strength and nature of the coupling between them. Here we discuss the strength of the interaction between the core and the 2n system in terms of particle-surface (phonon) coupling as a metric to establish whether the halo can be considered "weakly" or "strongly" coupled.

As discussed in detail by Bohr and Mottelson [21, 22], the strength of the particle-vibration (surface) coupling for quadrupole modes, specifically relevant to the present discussion, is given by:

$$f_{\lambda=2} = \left(\frac{5}{16\pi}\right)^{1/2} \left(\frac{\hbar\omega_2}{2C_2}\right)^{1/2} \frac{\langle k_2 \rangle}{\hbar\omega_2} \qquad (1)$$

where C_2 is the quadrupole restoring force parameter, $\hbar\omega_2$ is the vibration frequency, and $k_2(r) = R\ \partial V/\partial R$ the single-particle form factor, where we take R as the core radius r_c. In turn we have:

$$B(E2, 0^+ \rightarrow 2^+) = 5\left(\frac{3}{4\pi} ZeR^2\right)^2 \frac{\hbar\omega_2}{2C_2}$$

Values of $f_{\lambda=2}$ greater than unity are associated with strong coupling while values of $f_{\lambda=2}$ less than unity are associated with weak coupling. The softness of the surface quadrupole vibration/phonon mode is related to the C_2 coefficient, or the $B(E2)$, and the frequency $\hbar\omega_2$.* We estimate the single-particle form-factor, $\langle k_2 \rangle$, with a wavefunction approximated as a constant within the potential and an exponential tail outside, the decay constant of which depends on the $2n$ separation energy. The coupling is seen to decrease as the orbit becomes less bound. In turn, the overall dependence of $f_{\lambda=2}$ shown in Fig. 2 also decreases with the tunneling parameter $\mathscr{X}$. The curves represent the two cases that can be associated with a soft- and a hard core as indicated by the $B(E2)$ strengths in W.U. For the range of BE expected for ^{40}Mg, $f_{\lambda=2}$ is below unity for a $B(E2)$ of 10 W.U., signaling a regime where weak particle-surface coupling dominates, in contrast to the strong coupling expected in the lighter (more bound) even-A magnesium isotopes from ^{32}Mg to ^{38}Mg. A consequence of the weak coupling between the deformed core and the

* In this context, for example, the ^{9}Li core in ^{11}Li can be considered to be "soft", whereas the ^{4}He core in ^{6}He is "hard".

neutron halo is that the latter can be considered spherical to all practical purposes.

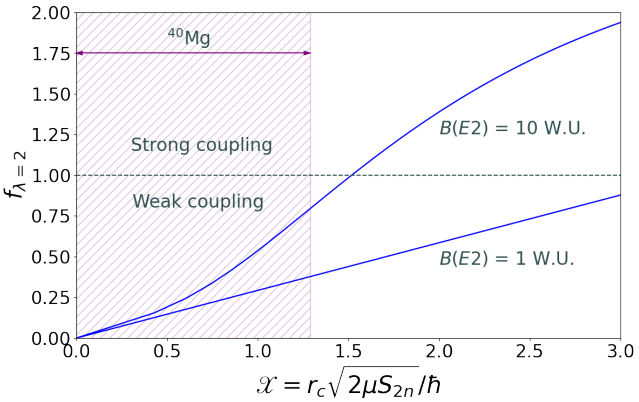

FIG. 2: Bohr-Mottelson particle-surface quadrupole coupling form factor, $f_{\lambda=2}$, as a function of $\mathcal{X}$. Two cases are shown, corresponding to soft- and hard- cores as represented by the given $B(E2)$ strength in single-particle units.

In the following we apply a phenomenological Weak Coupling Model [11] and the Particle-Rotor Model [12] to describe the spectrum of states that can arise in such a system, and when comparing results to experimental data in ^{40}Mg we assume that the γ-ray transitions of 500(14) keV and 670(16) keV correspond to the energies of the first and second 2^+ states, such that $2^+_1 \rightarrow 0^+_1 =$ 500 keV and $2^+_2 \rightarrow 0^+_1 = 670$ keV (see Refs. [5, 23]).

A. Weak Coupling Phenomenological Model

The coupling of a two neutron halo (e.g. νp^2) to a core is schematically illustrated in Fig. 3 and the phenomenological Hamiltonian describing the relevant degrees of freedom of the total system can be written as:

$$H(A+2) = H(A) + V_{nn} + V_{nn-core} \qquad (2)$$

The unperturbed energies of the core and two neutron subsystems are given by $H(A)$ and V_{nn} respectively, and $V_{nn-core}$ is the interaction between them.

It is natural to expect that effects of weak binding on excited states will show when the energy scales of the two degrees of freedom become comparable:

$$E_{core}(2^+) \approx E_{2n}(2^+) \qquad (3)$$

As discussed in appendix A, ^{40}Mg is one of few cases where this condition may be satisfied for p neutrons outside a deformed core.

It is interesting to note the recent work in Ref. [24], where the authors analyze the $2n$ decay mode of the 2^+_1 resonant state of ^{6}He. They show that the calculated double-differential breakup cross section for the ^{6}He + ^{12}C reaction at 240 MeV/nucleon will have a shoulder peak which comes from the $2n$ configuration in a νp^2 2^+ state.

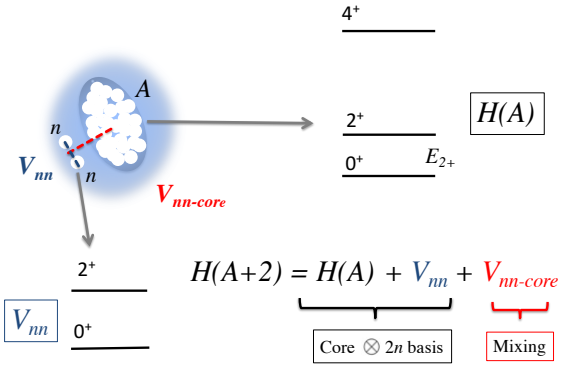

FIG. 3: Sketch of our weak-coupling approach to treat the mixing of the rotational core and the two neutrons degrees of freedom, where the matrix element $V_{nn-core}$ is anticipated to be small in comparison to the characteristic energies of the 2^+ of the core and the V_{nn} in the $\nu p^2_{3/2}$ configuration.

1. State Energies and Wavefunctions

The formation of a neutron halo is limited to weakly bound low-ℓ s and p orbits and the maximum spin for a two neutron halo system is then 2^+. For the lowest states in the scenario above, namely the 2^+ states, this results in a 2×2 matrix that can be studied as a function of the 2n binding energy.

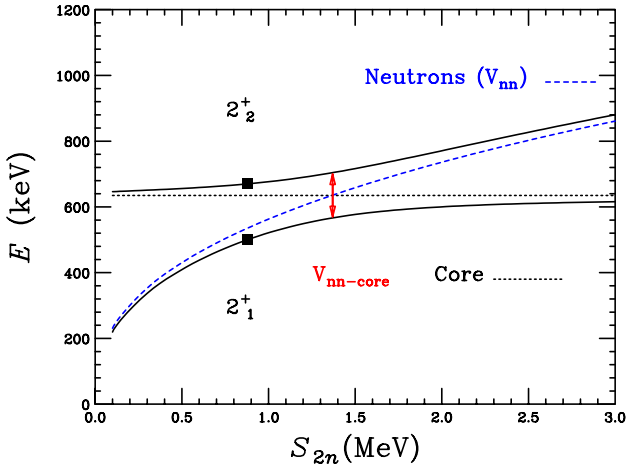

FIG. 4: Results of the weak coupling phenomenological model vs. S_{2n} for the case of a νp orbit (dashed blue line). The experimental energies are shown as black squares at the minimization solution. The two-body matrix element V_{nn} is assumed to scale with volume from ^{50}Ca.

The results of the diagonalization for the 2^+ state matrix vs. 2n separation energy are shown in Fig. 4 using the example of ^{40}Mg. In choosing the initial parameters we consider that the core unperturbed energy, $E_{core}(2^+)$, is that of ^{38}Mg and does not depend on the

neutron binding (dashed black line). The energy of the 2^+ neutron excitation, V_{nn}, has been scaled by volume from that in ^{50}Ca ($\nu p^2_{3/2}$ outside of ^{48}Ca) and as expected, decreases with S_{2n} (dashed blue line). It is interesting to see that the unperturbed lines cross for binding energies in the range expected for ^{40}Mg and even a small mixing matrix element $V_{nn-core}$ will give rise to largely mixed states in the laboratory frame. A minimization procedure on the experimental energies of the two potential states populated [5] gives a solution with $V_{nn-core}$ = 69keV, S_{2n}=877 keV, and wavefunctions:

$$\begin{aligned} |2^+_1\rangle &= 0.89|2^+_{core}\rangle + 0.45|2^+_{2n}\rangle \\ |2^+_2\rangle &= -0.45|2^+_{core}\rangle + 0.89|2^+_{2n}\rangle \end{aligned} \quad (4)$$

The fact that $V_{nn-core} \ll E_{core}(2^+)$ (V_{nn}) in this solution supports the weak coupling assumption.

2. Reaction Cross Section

The wavefunctions of the two 2^+ states (see Eq. 4) can also be used to determine their relative intensities populated in a direct knockout reaction using the procedure described in Refs. [25–27] and compared to that observed [5]. The cross-section to populate a given state in a direct reaction depends on the overlap of the initial and final state wavefunctions and may therefore be sensitive to the effects of weak binding.

To calculate the population of the final states in ^{40}Mg produced from the ^{41}Al-1p reaction we assume that the ground state of ^{41}Al is $K = 5/2^+$, from the $\pi[202]5/2$ Nilsson level originating from the $d_{5/2}$ spherical level. In the single-j approximation the collective spectroscopic factors follow the values of the Clebsch-Gordan coefficients: $\langle \frac{5}{2}\frac{5}{2}\frac{5}{2} - \frac{5}{2}|I_f 0\rangle$. In the minimization procedure we also include a single-particle spectroscopic factor $S_{sp}(5/2^+ \rightarrow 2^+_{2n})$ with a fitted value of 0.14. This gives a measure of the component of the $|2^+_{2n}\rangle$ state in the ground state of ^{41}Al. A good agreement with the observed relative population of the states as determined from the γ-ray intensities [5] with the assumption of parallel decays can be seen in Fig. 5.

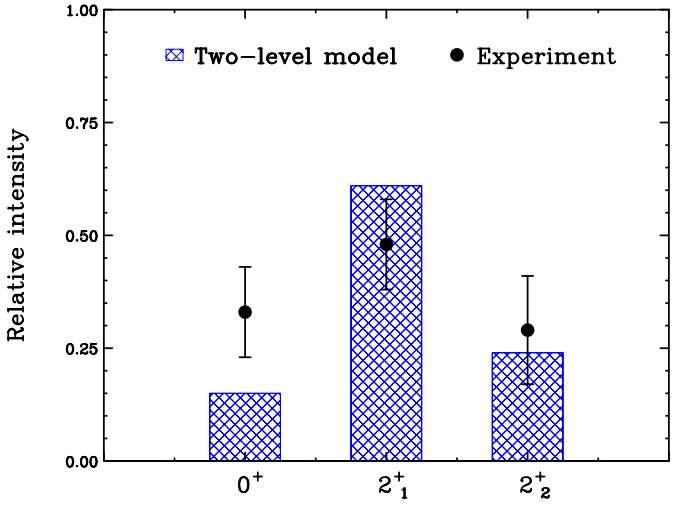

FIG. 5: Minimization results for the intensity ratio of the 2^+_1 and 2^+_2 states populated in the experiment.

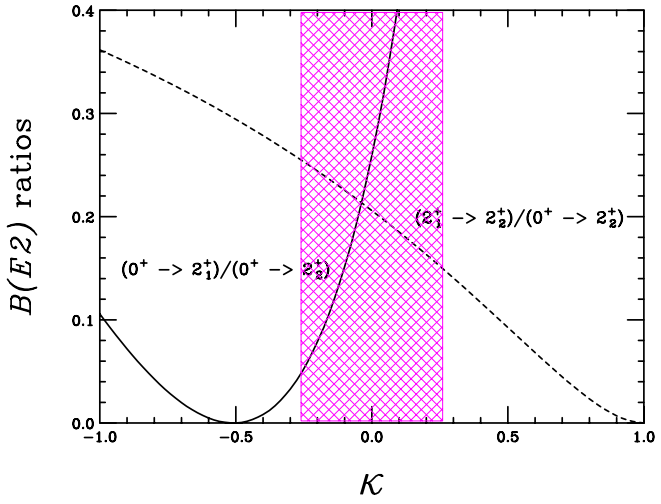

FIG. 6: Ratios of $B(E2)$s for the $0^+ \rightarrow 2^+_1$ and $2^+_1 \rightarrow 2^+_2$ transitions to the $0^+ \rightarrow 2^+_2$, as a function of the parameter κ. The (magenta) shaded region indicates the expected range for the values of κ.

3. Transition Probabilities

No data currently exists on $E2$ transition probabilities ($B(E2)$s) to low-lying states in a halo nucleus and it is interesting to consider the contribution of the neutron halo to excite the 2^+_1 and 2^+_2 states, for example in an intermediate energy Coulomb excitation experiment [28].

In the weak coupling framework we can calculate the $B(E2)'s$ and find the ratios to excite the 2^+_1 and 2^+_2 states:

$$\frac{B(E2, 0^+ \rightarrow 2^+_1)}{B(E2, 0^+ \rightarrow 2^+_2)} \approx \frac{(\alpha + \beta\kappa)^2}{(-\beta + \alpha\kappa)^2} \quad (5)$$

$$\frac{B(E2, 2^+_1 \rightarrow 2^+_2)}{B(E2, 0^+ \rightarrow 2^+_2)} \approx \frac{(\alpha(1-\kappa))^2}{(1-(\alpha/\beta)\kappa)^2} \quad (6)$$

where $\kappa = \langle 0^+|\mathscr{M}(E2)_{2n}|2^+_{2n}\rangle / \langle 0^+|\mathscr{M}(E2)_{core}|2^+_{core}\rangle = \langle 2^+_{2n}|\mathscr{M}(E2)_{2n}|2^+_{2n}\rangle / \langle 2^+_{core}|\mathscr{M}(E2)_{core}|2^+_{core}\rangle$, and α (=0.89) and β (=0.45) are the amplitudes in Eq. 4. These ratios are shown in Fig. 6, and we note that they are sensitive to the halo ($2n$) contribution. We may anticipate that the $2n$ matrix element will be of order one

single-particle unit or smaller depending on the effective charge acquire by the neutrons. In turn, the $B(E2)$ of ^{38}Mg should be similar to that of ^{36}Mg [29], $\approx$ 14 W.U. Thus, the shaded region indicates the expected range for κ, estimated from the values above. It is worth pointing out that from these results, the branching ratio $(2_2^+ \rightarrow 2_1^+)$ for a 170 keV transition from the assumed 670 keV state is expected to be small.

Although perhaps more experimentally ambitious, the magnetic moment of the 2_1^+ state can also provide a sensitive measurement of the $2n$ contribution since its gyro-magnetic factor is:

$$g(2_1^+) = \alpha^2 \frac{Z}{A} + \beta^2 \frac{1}{2} g_{s,\nu} \tag{7}$$

giving $g(2_1^+) \approx -0.14\ \mu_N$.

B. Particle-Rotor Model

The Particle-Rotor Model [12] has been used extensively to describe the coupling and alignment of valence nucleons outside a deformed core. Within this framework, the backbending phenomenon [30] was explained by Stephens [31] as a result of the crossing of the ground state (*gs* or *yrast*) band with an excited aligned band carrying single-particle angular momenta usually referred to as the *s* or *yrare* band. This can be simply understood by looking at the energies of the two bands as a function of angular momentum:

$$E_{gs} \approx \frac{\hbar^2}{2\mathscr{I}} I^2 \tag{8}$$

and

$$E_s \approx \frac{\hbar^2}{2\mathscr{I}} (I - 2j)^2 + 2\Delta \tag{9}$$

where for simplicity we assume that the two bands have equal moments of inertia, $\mathscr{I}$. At a critical angular momentum, I_c, the extra energy (2Δ) required to break the pair is compensated by the loss of rotational energy due to the contribution, $2j$, of the aligned particles to the total spin. An estimate from Eqs. 8 and 9 gives:

$$I_c \approx j + \frac{3\Delta}{j^2 E_{2^+}} \tag{10}$$

Typically, in the rare earth, these crossings occur at relatively high-spins, while here it is anticipated to be at low-spin.

In order to apply this scenario to the case of a deformed weakly bound nucleus we first look at the ^{38}Mg *yrast* band and, assuming the maximum alignment of $2j = 2$ for the $p_{3/2}$ level, we adjust the Coriolis mixing matrix element to reproduce the observed energies of the $I = 2^+$ and $I = 4^+$ levels in ^{38}Mg (Fig. 7 bottom panel) from the crossing of the *gs* (dashed line) and *s* bands (dotted line).

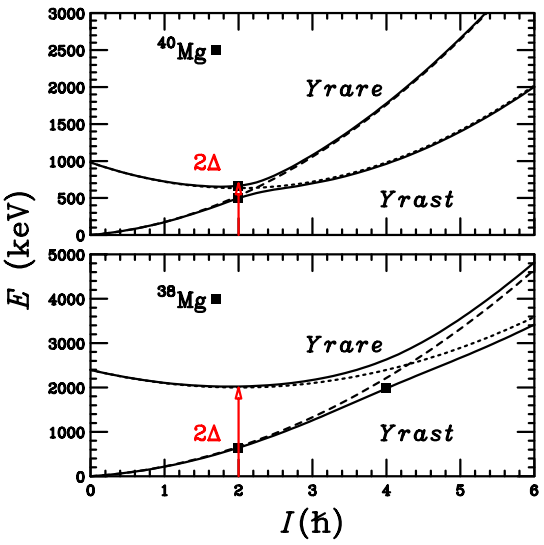

FIG. 7: Band-crossing scenario applied to both ^{38}Mg (bottom) and ^{40}Mg (top) showing the need for a quenched gap in ^{40}Mg (red arrows) that can be attributed to the weak binding of the $p_{3/2}$ orbital. The *gs* and *s* bands are shown by the dash and dotted lines respectively

For ^{40}Mg, we consider the 2_1^+ and 2_2^+ to belong to the *gs* (*yrast*) and *s* (*yrare*) bands respectively. Assuming the same Coriolis matrix element for ^{40}Mg as derived for ^{38}Mg, the similarity in their energies requires a reduced pairing gap to $2\Delta \approx 0.75$ MeV, which is half of that in ^{38}Mg (Fig. 7 top panel) to reproduce the data. That is, the energy to break a neutron $p_{3/2}$ pair in ^{40}Mg needs to be reduced, which is suggestive of a quenched pairing due to the reduced overlap induced by the weak binding, this quenching is consistent with the volume overlap shown in Fig. 1. It is worth pointing out that with the parameters above, a *backbend* in angular momentum vs. rotational frequency is predicted for ^{40}Mg.

IV. CONCLUSION

While the phenomenon of one- and two-neutron ground-state halo nuclei is well established, the effects of weak binding on the low-lying excitation spectrum remain largely unexplored. To address this interesting question we have studied the coupling of weakly bound (halo) valence neutrons to a deformed core using a Weak-Coupling phenomenological approach and the Particle-Rotor model. A "universal"plot that relates the $2n$ separation energy (S2n) to the volume overlap between the core and halo was used to characterize and identify possible halo nuclei. We illustrated our results using the known properties of ^{38,40}Mg to discuss the impact of weak binding on the low lying excitation spectrum, one proton removal reaction cross-sections and transition probabilities. Despite its simplicity, our phe-

nomenological model captures the main physical ingredients and provides a framework that allows us to to examine possible coupling schemes involving a core and halo.

Of course, other approaches to the structure of ^{40}Mg exist [32, 33] that differ in the nature of the second experimental γ transition. It is clear that further experimental and theoretical works will be required to elucidate their intriguing structure, which we trust will be motivated by this work.

Acknowledgments

This material is based upon work supported by the U.S. Department of Energy, Office of Science, Office of Nuclear Physics under Contract No. DE-AC02-05CH11231. AP's work is supported in part by the Ministerio de Ciencia, Innovación y Universidades (Spain), Severo Ochoa Programme SEV-2016-0597 and grant PGC-2018-94583.

V. APPENDIX A

The condition that the energy scales of the two degrees of freedom within in weakly bound system are comparable

$$E_{core}(2^+) \approx E_{2n}(2^+) \tag{11}$$

can be used to signal cases when the observed spectrum of states may by modified by the interaction of the halo and core, as discussed in the main text. To do this we first rewrite this condition explicitly for a deformed rotor and assume the energy of the two neutron 2^+ is given by a modified gap,

$$\frac{2(2+1)\hbar^2}{2\mathscr{I}} \approx \frac{2}{3}(2\widetilde{\Delta}_{2n}) \tag{12}$$

where the 2/3 factor is an empirical estimate that takes into account the fact that 2^+ two-particle states are lower than the pairing gap due to the quadrupole interaction. The moment of inertia is a function of the mass number, the deformation and the pairing gap [34]. We use a pairing gap (in MeV):

$$\Delta \approx \frac{7.36}{A^{1/3}}(1 - 8.15(N-Z)^2/A^2) \tag{13}$$

derived from the fits in Ref. [35]. From the discussions in Section II we estimate $\widetilde{\Delta}_{2n}$ by modifying the expression above by a volume correction associated to the weakly bound neutrons and obtain:

$$\frac{\hbar^2}{\mathscr{I}(A,\epsilon,\Delta)} \approx 0.44\Delta(\langle r_c^2\rangle/\langle r^2\rangle)^{3/2} \tag{14}$$

where $\langle r^2\rangle$ depends on S_{2n} through the tunneling parameter $\mathscr{X}$. For a given deformation ϵ we can solve for the locus points in the nuclear chart, (A, N, Z), that satisfy Eq. (14) and where a *transition* to a weakly bound "*phase*" might occur. This solution is perhaps relevant only for p orbits, the lowest (ℓ, j) from which a 2^+ excitation could be built and for which the low centrifugal barrier still allows the formation of a halo. The result, obtained for a notional $\epsilon = 0.4$, limits the accessible region of interest to light masses, with that near ^{40}Mg being the heaviest that can be reached, while heavier candidates are likely to be beyond the reach of all planned experimental facilities.

[1] I. Tanihata, H. Hamagaki, O. Hashimoto, Y. Shida, N. Yoshikawa, K. Sugimoto, O. Yamakawa, T. Kobayashi, and N. Takahashi, Phys. Rev. Lett. **55**, 2676 (1985), URL https://link.aps.org/doi/10.1103/PhysRevLett.55.2676.

[2] P. G. Hansen and B. Jonson, **4**, 409 (1987), URL https://doi.org/10.1209/0295-5075/4/4/005.

[3] A. B. Migdal, Sov. J. Nucl. Phys. **16**, 238 (1973), [Yadernaya Fizika **16**(2), 427-434 (1972)].

[4] F. Barranco, P.F. Bortignon, R.A. Broglia, G. Colò, and E. Vigezzi, Eur. Phys. J. A **11**, 385 (2001), URL https://doi.org/10.1007/s100500170050.

[5] H. L. Crawford, P. Fallon, A. O. Macchiavelli, P. Doornenbal, N. Aoi, F. Browne, C. M. Campbell, S. Chen, R. M. Clark, M. L. Cortés, et al., Phys. Rev. Lett. **122**, 052501 (2019), URL https://link.aps.org/doi/10.1103/PhysRevLett.122.052501.

[6] E. Caurier, F. Nowacki, and A. Poves, Phys. Rev. C **90**, 014302 (2014), URL https://link.aps.org/doi/10.1103/PhysRevC.90.014302.

[7] I. Hamamoto, Phys. Rev. C **76**, 054319 (2007), URL https://link.aps.org/doi/10.1103/PhysRevC.76.054319.

[8] H. Nakada and K. Takayama, Phys. Rev. C **98**, 011301 (2018), URL https://link.aps.org/doi/10.1103/PhysRevC.98.011301.

[9] K. Fossez, J. Rotureau, N. Michel, Q. Liu, and W. Nazarewicz, Phys. Rev. C **94**, 054302 (2016), URL https://link.aps.org/doi/10.1103/PhysRevC.94.054302.

[10] K. Fossez, W. Nazarewicz, Y. Jaganathen, N. Michel, and M. Płoszajczak, Phys. Rev. C **93**, 011305 (2016), URL https://link.aps.org/doi/10.1103/PhysRevC.93.011305.

[11] A. Arima and I. Hamamoto, Annual Review of Nuclear Science **21**, 55 (1971), https://doi.org/10.1146/annurev.ns.21.120171.000415, URL https://doi.org/10.1146/annurev.ns.21.120171.000415.

[12] S. G. Nilsson and I. Ragnarsson, *Shapes and Shells in Nuclear Structure* (Cambridge University Press, 1995).

[13] P. G. Hansen, A. S. Jensen, and B. Jonson, Annual

Review of Nuclear and Particle Science **45**, 591 (1995), https://doi.org/10.1146/annurev.ns.45.120195.003111, URL https://doi.org/10.1146/annurev.ns.45.120195.003111.

[14] K. Riisager, A. Jensen, and P. Møller, Nuclear Physics A **548**, 393 (1992), ISSN 0375-9474, URL https://www.sciencedirect.com/science/article/pii/037594749290691C.

[15] K. Riisager, **T152**, 014001 (2013), URL https://doi.org/10.1088/0031-8949/2013/t152/014001.

[16] A. S. Jensen, K. Riisager, D. V. Fedorov, and E. Garrido, **61**, 320 (2003), URL https://doi.org/10.1209/epl/i2003-00172-5.

[17] V. S. Bhasin and I. Mazumdar, *Few Body Dynamics, Efimov Effect and Halo Nuclei* (Springer, Cham, 2021), ISBN 978-3-030-56170-3.

[18] A. Ozawa, T. Suzuki, and I. Tanihata, Nuclear Physics A **693**, 32 (2001), ISSN 0375-9474, radioactive Nuclear Beams, URL https://www.sciencedirect.com/science/article/pii/S0375947401011526.

[19] W. Huang, M. Wang, F. Kondev, G. Audi, and S. Naimi, **45**, 030002 (2021), URL https://doi.org/10.1088/1674-1137/abddb0.

[20] M. Wang, W. Huang, F. Kondev, G. Audi, and S. Naimi, **45**, 030003 (2021), URL https://doi.org/10.1088/1674-1137/abddaf.

[21] A. Bohr and B. Mottelson, Dan. Mat. Fys. Medd. **27** (1953).

[22] A. Bohr and B. R. Mottelson, *Nuclear Structure, Volume II: Nuclear Deformations* (World Scientific Publishing Co. Pte. Ltd., Singapore, 1999).

[23] H. L. Crawford, P. Fallon, A. O. Macchiavelli, R. M. Clark, B. A. Brown, J. A. Tostevin, D. Bazin, N. Aoi, P. Doornenbal, M. Matsushita, et al., Phys. Rev. C **89**, 041303 (2014), URL https://link.aps.org/doi/10.1103/PhysRevC.89.041303.

[24] Shoya Ogawa and Takuma Matsumoto, arXiv:2111.04285 [nucl-th] (2021).

[25] B. Elbek and P. O. Tjøm, *Advances in Nuclear Physics* (Springer, Boston, MA, 1969), chap. Single Nucleon Transfer in Deformed Nuclei, pp. 259–323, ISBN 978-1-4757-9020-7.

[26] A. O. Macchiavelli, H. L. Crawford, C. M. Campbell, R. M. Clark, M. Cromaz, P. Fallon, M. D. Jones, I. Y. Lee, A. L. Richard, and M. Salathe, Phys. Rev. C **96**, 054302 (2017), URL https://link.aps.org/doi/10.1103/PhysRevC.96.054302.

[27] A. O. Macchiavelli, H. L. Crawford, C. M. Campbell, R. M. Clark, M. Cromaz, P. Fallon, M. D. Jones, I. Y. Lee, and M. Salathe, Phys. Rev. C **97**, 011302 (2018), URL https://link.aps.org/doi/10.1103/PhysRevC.97.011302.

[28] T. Glasmacher, Annual Review of Nuclear and Particle Science **48**, 1 (1998), https://doi.org/10.1146/annurev.nucl.48.1.1, URL https://doi.org/10.1146/annurev.nucl.48.1.1.

[29] P. Doornenbal, H. Scheit, S. Takeuchi, N. Aoi, K. Li, M. Matsushita, D. Steppenbeck, H. Wang, H. Baba, E. Ideguchi, et al., Phys. Rev. C **93**, 044306 (2016), URL https://link.aps.org/doi/10.1103/PhysRevC.93.044306.

[30] A. Johnson, H. Ryde, and J. Sztarkier, Physics Letters B **34**, 605 (1971), ISSN 0370-2693, URL https://www.sciencedirect.com/science/article/pii/037026937190150X.

[31] F. Stephens and R. Simon, Nuclear Physics A **183**, 257 (1972), ISSN 0375-9474, URL https://www.sciencedirect.com/science/article/pii/0375947472906586.

[32] N. Tsunoda, T. Otsuka, K. Takayanagi, N. Shimizu, T. Suzuki, Y. Utsuno, S. Yoshida, and H. Ueno, Nature **587**, 66 (2020), URL https://doi.org/10.1038/s41586-020-2848-x.

[33] Y. Suzuki and M. Kimura, Phys. Rev. C **104**, 024327 (2021), URL https://link.aps.org/doi/10.1103/PhysRevC.104.024327.

[34] A. Migdal, Nuclear Physics **13**, 655 (1959), ISSN 0029-5582, URL https://www.sciencedirect.com/science/article/pii/0029558259902640.

[35] A. Jensen, P. Hansen, and B. Jonson, Nuclear Physics A **431**, 393 (1984), ISSN 0375-9474, URL https://www.sciencedirect.com/science/article/pii/0375947484901167.